Applied Mathematics and Mechanics
(English Edition, Vol 24, No 8, Aug 2003)

Published by Shanghai University,
Shanghai, China

Article ID: 0253-4827(2003)08-0928-08

FLOW PROPERTIES OF A DUSTY-GAS POINT SOURCE IN A SUPERSONIC FREE STREAM *

WANG Bo-yi (王柏懿)[1], Alexander N. Osiptsov[2], Misha A. Teverovshii[2]

(1. LNM, Institute of Mechanics, Chinese Academy of Sciences,
Beijing 100080, P.R.China;
2. Institute of Mechanics, Lomonosov Moscow State University,
Moscow 119899, Russia)

(Communicated by BIAN Yin-gui, Original Member of Editorial Committee, AMM)

Abstract: *By using Lagrangian method, the flow properties of a dusty-gas point source in a supersonic free stream were studied and the particle parameters in the near-symmetry-axis region were obtained. It is demonstrated that fairly inertial particles travel along oscillating and intersecting trajectories between the bow and termination shock waves. In this region, formation of "multi-layer structure" in particle distribution with alternating low- and high-density layers is revealed. Moreover, sharp accumulation of particles occurs near the envelopes of particle trajectories.*

Key words: dusty gas; supersonic flow; point source; particle inertia; trajectory intersection; multi-layer structure

Chinese Library Classification: O359 **Document code**: A
2000 Mathematics Subject Classification: 76T15

Introduction

Dusty-gas, as a two-phase medium, is the suspension of particles and gas, which are known as dispersed and carrier phase respectively. For such a system, relaxation process happens due to great mass difference between the particle and gas molecule. In many dusty-gas flows, the trajectories of inertial particle may be oscillating, which results in appearance of regions with multiple intersections of the particle trajectories[1]. Numerical modeling of these effects are of great significance in various naturally-occurring phenomena and practical engineering problems, for example, in astrophysics (evaporation from a comet nucleus to its atmosphere), aerospace engineering (flow from an under-expanded nozzle into oncoming flow), high technologies (drying powdered materials in colliding-jet-sprayers) and so on.

* **Received date**: 2002-03-19; **Revised date**: 2003-04-29

Foundation items: the National Natural Science Foundation of China (NSFC grant No. 90205024); the Russian Foundation for Basic Research (RFBR grant No. 02-01-00770); RFBR-NSFC grant No. 99-01-39020)

Biography: WANG Bo-yi (1941 ~), Professor (E-mail: wby@imech.ac.cn)

The study of two-phase flows with such regions requires the modification of the ordinary dusty-gas model where the single-valueness of the particle parameters is assumed [2]. It also necessitates the development of numerical algorithms, which allow to distinguish the boundaries of the regions with intersecting particle trajectories and to calculate correctly the particle concentration. Crowe and his co-authors[3,4] have been published comprehensive reviews on numerical methods of dilute gas-particle flows. Essentially, these methods fall into two categories: Lagrangian and Eulerian. For our problem, the Eulerian approach fails due to non-uniqueness of the dispersed phase parameters. However, the Lagrangian approach of applying a statistical averaging procedure to a large number of trajectories takes heavy computation costs. Therefore, in the literature, for calculating dust parameters in these regions, so-called "large-particle" method or its modifications are used most widely but hey often introduce to inadequate accuracy in the particle concentration. Osiptsov[5] suggested a novel approach for calculating the dispersed phase density, using the Lagrange form of the particle continuity equation. Recently, Healy and Young[6] calculated some 2-D examples to assess the Ositpsov method and concluded that it is more elegant and efficient than the traditional Lagrangian method. The present paper improves the novel Lagrangian method and illustrates its application to the dusty-gas flows with multiple trajectory intersection. This method makes it possible to investigate these two-phase systems where the particle concentration distributions have a multi-layer structure with sharp accumulation near the trajectory envelopes.

1 Problem Formulation

As a typical problem, we consider a steady flow resulted due to the interaction of a supersonic dusty-gas point source with a hypersonic flow of a pure-gas. The flow diagram is shown in Fig. 1, where the dusty-gas source with a constant mass flow rate of carrier phase Q^* is located at point O_1 and the pure-gas has a free stream velocity V_∞^* in the direction of negative axis $O_2y_2^*$ (Below, an asterisk denotes the dimensional quantities when necessary). In the flow from the source, the termination shock wave 1 appears while the bow shock wave 2 forms in the oncoming flow. The inner and outer shock layers are separated by the contact surface 3. We assume that, prior to the termination shock wave, the gas reaches to the maximum speed V_{max}^* and the particles are in equilibrium with the carrier phase. Hence, the particle inertia manifests itself behind the shock front 1. The particle motion is considered in the curvilinear coordinates (x^*, y^*) directed along and in the normal to the termination shock surface. Concerning the dispersed phase, we adopt the usual assumptions for a dilute dusty gas[7]: the particles are non-deformable spheres with uniform diameter d and mass m, the Brownian motion is ignored, and the volume

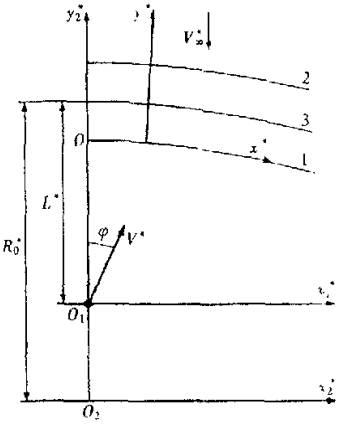

Fig. 1 Flow diagram

fraction or mass concentration of the particles are small enough to neglect their effects on the carrier phase. Concerning the carrier phase, we assume that the colliding gases are perfect with the constant parameters of the adiabatic curve γ_1 and γ_2, respectively.

In such a one-way-coupling problem of two-phase flow, we obtain the following expressions for discontinuity geometry by using thin shock layer approximation of the pure gas[8]:

a) The distance from the source to the stagnation point:

$$L^* = [((\gamma_1 + 1)/8\pi\gamma_1)^{1/2} Q^* V^*_{max}/\rho^*_\infty V^{*2}_\infty]^{1/2}. \tag{1}$$

b) The curvature radius of the contact surface at the stagnation point:

$$R_0^* = 3L^*/2. \tag{2}$$

c) The thickness of the shock layer 1:

$$\delta_1^* = \varepsilon_1 R_0^* (\sqrt{a} - b)/(a - b^2). \tag{3}$$

Here $\varepsilon_1 = (v_{1c}/V^*_\infty)(\rho_{1c}/\rho^*_\infty)^{1/2}$, $a = 2$, $b = 0.5(\rho^*(0)/\rho^*_{1c})^{-1/2}$, where the subscript $1c$ denotes the parameters behind the shock 1 on the symmetry axis and $\rho^*(0)$ is the gas density prior to the shock 1 on the symmetry axis.

d) The thickness of the shock layer 2:

$$\delta_2^* = \kappa_2 R_0^*/(1 + (8\kappa_2/3)^{1/2}). \tag{4}$$

Here $\kappa_2 = (\gamma_2 - 1)/(\gamma_2 + 1)$.

e) The form of the contact surface in the polar coordinates (r^*, φ):

$$r^* = L^* \varphi/\sin\varphi. \tag{5}$$

Similarly, the approximate formulas for the gas parameters between the bow and termination shock waves in the neighborhood of the symmetry axis can be determined analytically based on supersonic flow theory[9,10] and they are not reproduced here due to awkwardness.

To obtain the solution of the particle parameters (denoted by the subscript s), it is convenient to introduce the nondimensional variables:

$$x = x^*/R_0^*, \quad y = y^*/\kappa_2 R_0^*, \quad R = R^*/R_0^*, \quad r_s = r_s^*/R_0^*,$$
$$u_s = u_s^*/V_\infty^*, \quad v_s = v_s^*/V_\infty^*, \quad T_s = T_s^*/T_{02}^*, \quad \rho_s = \rho_s^*/\rho_s^*(0).$$

Here T_{02}^* and $\rho_s^*(0)$ are respectively the stagnation temperature and the particle density on the symmetry axis prior to the shock front 1. Due to the curvilinear coordinates, $R(x)$ and $r_s(x)$, which are the curvature radius and the distance from the symmetry axis to the surface of the shock wave 1 respectively, appear in the governing equations.

In the nondimensional Lagrange coordinates (x_0, t), where x_0 is the initial position of a given particle trajectory on the shock wave 1 and $t = t^* V_\infty^*/R_0^*$ is the motion time of the particle from its initial position, the dispersed phase equations of motion and energy take the following form:

$$\begin{cases} \dfrac{\partial x_s}{\partial t} = \dfrac{u_s}{1 + H}, \quad \dfrac{\partial y_s}{\partial t} = \dfrac{v_s}{\kappa_2}, \\ \dfrac{\partial u_s}{\partial t} = \beta\mu D(u - u_s) - \dfrac{u_s v_s}{RH}, \\ \dfrac{\partial v_s}{\partial t} = \beta\mu D(v - v_s) - \dfrac{u_s^2}{RH}, \\ \dfrac{\partial T_s}{\partial t} = \dfrac{2C}{3Pr}\beta\mu G(T - T_s). \end{cases} \tag{6}$$

In the equations above, $H = 1 + \kappa_2 y_s / R$ is Lame's coefficient, $\beta = 3\pi d \mu_{02}^* R_0^* / m V_\infty^*$ the relaxation parameter (here μ_{02}^* is the viscosity of the gas 2 at the stagnation point), $C = c_{p2}/c_s$ the specific heat ration of the gas 2 and particle material, Pr the gas Prandtl number while $\mu = \mu^* / \mu_{02}^*$ is the nondimensional gas viscosity. In this paper, we assume that dependence of viscosity on temperature takes the exponential form $\mu = T^\omega$. Besides, D and G are the correction functions for the interphase transfer of momentum and heat[11]:

$$\begin{cases} D = \left(1 + \frac{1}{6} Re_s^{2/3}\right)\left(1 + \exp\left(-\frac{0.427}{Ma_s^{4.63}}\right)\right), \\ G = (1 + 0.3 Pr^{1/3} Re_s^{1/2}) \Big/ \left(1 + 3.42 \frac{Ma_s}{Re_s} \frac{1 + 0.3 Pr^{1/3} Re_s^{1/2}}{Pr}\right). \end{cases} \tag{7}$$

Here $Re_s = \rho^* \mid V^* - V_s^* \mid d / \mu^*$ is the slip Reynolds number of the particle and Ma_s is the Mach number of the flow past the particle. Obviously, these expressions take into account the finiteness of the Reynolds number, Mach number and Knudsen number of the gas flow around the particle. It should be pointed out that the gas velocity and temperature (u, v and T) in Eq.(6) are nondimensional variables similar to those for the partcles while gas density ρ^* is scaled to ρ_∞^*.

2 Lagrangian Method

As well-known, the continuity equation of the dispersed phase in the curvilinear Euler coordinates (x, y) fitted to the termination shock wave is written as:

$$\frac{\partial(\rho_s u_s r_c)}{\partial x} + \frac{1}{\kappa_2} \frac{\partial(\rho_s v_s r_c H)}{\partial y} = 0. \tag{8}$$

The corresponding equation in the Lagrange coordinates (x_0, t) can be easily obtained

$$\rho_s(x_0, t) \mid J \mid = \frac{r_c(x_0)}{r_s(x_s, y_s)} \rho_s(x_0, 0). \tag{9}$$

Here J is the Jacobian of transformation from the Euler coordinates to the Lagrange coordinates:

$$J = \left(1 + \frac{\kappa_2 y_s}{R}\right) \frac{v_s(x_0, t)}{v_s(x_0, 0)} \frac{\partial x_s(x_0, t)}{\partial x_0} - \frac{u_s(x_0, t)}{v_s(x_0, 0)} \frac{\partial y_s(x_0, t)}{\partial x_0}. \tag{10}$$

Eq.(9) gives the relation between the initial and current values of the dispersed phase density, $\rho_s(x_0, 0)$ and $\rho_s(x_0, t)$, along a fixed particle trajectory $(x_s(x_0, t), y_s(x_0, t))$. In order to calculate the particle concentration at any instant of time, we should determine the functions $\partial x_s(x_0, t)/\partial x_0$ and $\partial y_s(x_0, t)/\partial x_0$ in relation (10) by differentiating the first four equations of (6) with respect to x_0:

$$\frac{\partial W_1(x_0, t)}{\partial t} = \frac{W_2}{H} + \frac{\kappa_2 u_s (y_s R' - R W_3)}{R^2 H^2}, \tag{11a}$$

$$\frac{\partial W_2(x_0, t)}{\partial t} = \beta\mu G\left(W_1 \frac{\partial u}{\partial x} + W_3 \frac{\partial u}{\partial y} - W_2\right) + \beta(u - u_s)(\mu G)' - u_s W_4 + \frac{v_s W_2}{RH} + \frac{u_s v_s (R' + \kappa_2 W_3)}{R^2 H^2}, \tag{11b}$$

$$\frac{\partial W_3(x_0,t)}{\partial t} = \frac{W_4}{\kappa_2}, \tag{11c}$$

$$\frac{\partial W_4(x_0,t)}{\partial t} = \beta\mu G\left(W_1\frac{\partial v}{\partial x} + W_3\frac{\partial r}{\partial y} - W_4\right) + \beta(v - v_s)(\mu G)' + \frac{2u_s W_2}{RH} - \frac{u_s^2(R' + \kappa_2 W_3)}{R^2 H^2}. \tag{11d}$$

Here the superscript "′" notes the derivative with respect to x_0, and the definitions of the four functions W are as follows:

$$W_1 = \frac{\partial x_s(x_0,t)}{\partial x_0},\quad W_2 = \frac{\partial u_s(x_0,t)}{\partial x_0},\quad W_3 = \frac{\partial y_s(x_0,t)}{\partial x_0},\quad W_4 = \frac{\partial v_s(x_0,t)}{\partial x_0}.$$

In this way, the problem of determination of the dispersed phase parameters is reduced to solving the system of ordinary differential equations (6), (11) and the relation (10) for various initial values x_0. For the calculations, required parameters of the carrier phase as well as their space derivatives are obtained from the thin shock layer approximation theory as described before. Based on the assumption of the equilibrium flow emitted from the dusty-gas point source, the initial conditions at the termination shock wave in the neighborhood of the symmetry axis can be given as:

$$t = 0:\ x_s = x_0,\quad y_s = 0,\quad u_s = 0.5x_0(\rho(0))^{-1/2},\quad v_s = (\rho(0))^{1/2},$$
$$T_s = T(0),\quad W_1 = 1,\quad W_2 = 0.5(\rho(0))^{1/2},\quad W_3 = W_4 = 0,\quad \rho_s = 1.$$

Here $\rho(0)$ and $T(0)$ are the nondimensional density and temperature of the gas prior to the termination shock wave. In addition, it is obtained from (5) that for small x_0: $R(x_0) = 1 + 1.5x_0^2$.

3 Numerical Results

From Eq. (6), it is known that the similarity criteria for the particles flow are β, Rb, c_{p1}/c_s, c_{p2}/c_s and Pr, where $Rb = Re_0^{2/3}/6$, and $Re_0 = \rho_\infty^* V_\infty^* d/\mu_{02}^*$ is the Reynolds number of the free stream based on the particle diameter. The numerical calculation of the problems (6), (10) and (11) were performed by the Kutta-Merson method for the flow media with the following properties: $\gamma_1 = \gamma_2 = 1.4$, $c_{p1}/c_{p2} = 1$, $\mu_{01}^*/\mu_{02}^* = 1$, $\omega_1 = \omega_2 = 0.5$, $c_{p1}/c_s = c_{p2}/c_s = 1$ and $Pr = 2/3$. The computation region along the generatrix of the termination shock wave is $0 \leqslant x \leqslant 0.4$ (in the neighborhood of the symmetry axis).

Typical calculation results of gas and particle motions for $Rb = 100$ are plotted in Fig. 2, where the solid lines 1 and 2 denote the contact surface and the bow shock wave respectively. The calculated gas streamlines (dashed lines) indicate that, due to the interaction between the oncoming free stream and the point source flow, the gases 1 and 2 deflect both and move aside. Due to the inertia effect, the particles do not immediately follow after the motion change of the carrier gas in the shock layers. For example, a heavy particle may move across the contact surface or even the bow shock wave. In our problem, velocity slip and temperature jump between the dispersed and carrier phases firstly appear behind the termination shock wave. In this non-

equilibrium state, the particles should exchange their momentum and energy with the gases. For particles of large inertia, it takes quite a long time to perform the relaxation process between the two phases. In the computations, we select two typical values for the inertia parameter: $\beta = 0.01$ for the large inertia particle and $\beta = 1$ for the small inertia particle. The calculated particle trajectories demonstrate that two kinds of particle motion may occur: oscillatory type (curve 3 for $\beta = 0.01$) and monotonic type (curve 4 for $\beta = 1$).

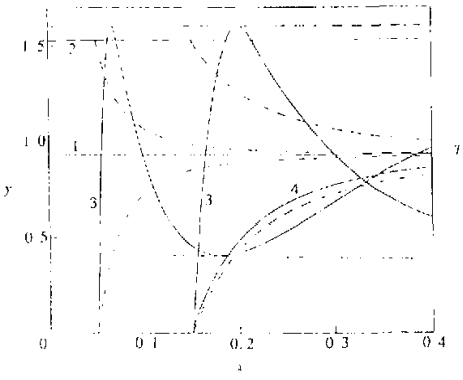

Fig.2 Gas streamlines and particle trajectories

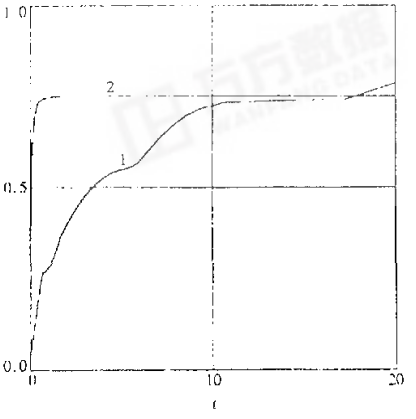

Fig.3 Particle temperature on the symmetry axis

Similar to the particle motion, depending on the inertia parameter β, different features may appear in the thermodynamic behavior of the particles. In Fig. 3, the time history of particle temperature is shown for the particle moving along the symmetry axis. Here $Rb = 100$ and $\beta = 0.01$ (for curve 1) or 1 (for curve 2). In our calculations, the stagnation temperature of the oncoming flow is greater than that of the source flow and then the cold particles are heated after they enter into the shock layers. As known above, the heavy particles ($\beta = 0.01$) can enter into the outer shock layer while the light particles ($\beta = 1$) move only inside the inner shock layer. Hence, the heavy particles can reach a higher temperature which is approaching the stagnation temperature. Moreover, the heating rate also depends on the kind of the particle trajectory. For the particles which perform the oscillations, the heating rate differs for different segments of the trajectory corresponding to the shock layer 1, 2 and the external or internal gas flows (see curve 1). In contrast to the heavy particles, the heating of the particles moving without oscillations occurs in the shock layer 1 at almost constant rate (see curve 2).

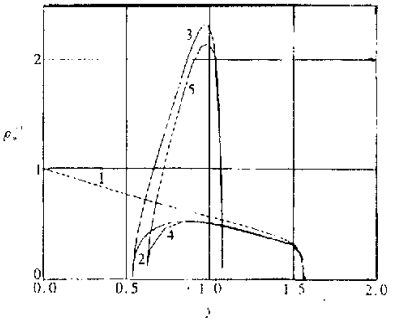

Fig.4 Particle concentration distributions

As mentioned above, by substituting the solutions of Eqs. (6) and (11) into the relation (10), the particle concentration can be determined. In Fig. 4, for the case of $Rb = 100$ and $\beta = 0.01$, we plotted the density of three particle continua which intersect the line $x = \text{const}$: (a) Before the first turn (see curve 1 ($x = 0, 0.1, 0.4$)); (b) After the first but before the second turn (see curves 2($x = 0, 0.1$) and 4 ($x = 0.4$)); (c) After the second but before the third turn (see curves 3 ($x = 0$) and 5 ($x = 0.4$)). The total density is the sum of the densities of each such continuum. As follows from the calculations, the contribution of the other continua of the particles to the total density may be ignored. It is seen from Fig. 4 that the particle distribution has a multi-layer structure with alternating low- and high-density layers, and near the envelopes of the particle trajectories, the particle concentration tends to infinite. In order to reveal the mechanism of the particle accumulation in detail, let us consider the oscillatory type of the particle motion first. It is seen from Fig. 2 that the particles with large inertia oscillate and intersect the contact surface several times. At the turn points, the normal velocity of the particles vanishes which results in an infinite particle density. In other words, the particles accumulate near the envelopes of the particle trajectories (chain lines). Between the accumulation regions there occur multiple intersections of the particle trajectories, which presents considerable difficulties of calculating the particle parameters in this region using the Euler approach. The Lagrangian method developed in this paper makes it possible to overcome these difficulties connected with non-uniqueness of the dispersed phase parameters. Of course, it should be noted that the neighborhood of the contact surface is also a region of the particle accumulation. This region exists for both two kinds of particle motion although it is the only possible accumulation mechanism for the monotonic motion case. The accumulation effect in the near-contact-surface region is weaker than that in the near-trajectory-envelope regions. The reason is that the normal velocity of the particle near the contact surface does not become zero except $x \to \infty$. Compared to the multiple accumulation case, for $Rb \in [0, 100]$, the single accumulation zone in the neighborhood of the contact surface exists over a much wider range of the inertia parameter β.

4 Conclusion

The novel Legrangian method for calculating the particle concentration was developed to predict the flow structure formed near the symmetry axis when a supersonic flow of a pure-gas collides with a supersonic flow from a dusty-gas point source. In the region between the bow and termination shock waves, the existence of zone with multiple intersections of the particle trajectories was detected. The formation of multi-layer structure in the particle distribution, where low- and high-density layer appear alternatively, was revealed. The effect of sharp accumulation and stratification of the dispersed phase in the shock layers may be of great importance for interpretation of experimental data on comet atmospheres and verious relevant phenomena.

References:

[1] Osiptsov A N, Shapiro E G. Two-phase mass injection on the nose of a blunt body in a hypersonic gas flow[J]. *Izv Ross Akad Nauk, Mekh Zhidk Gaza*, 1992, (4): 60 – 66. (in Russian)

[2] Marble F. Dynamics of dusty gases[J]. *Ann Rev Fluid Mech*, 1970, **2**: 397 – 446.

[3] Crowe C T. Review—numerical models for dilute gas-particle flows[J]. *Trans ASME, J Fluids Engineering*, 1982, **104**(3): 297 – 303.

[4] Crowe C T, Troutt T R, Chung J N. Numerical models for two-phase turbulent flows[J]. *Ann Rev Fluid Mech*, 1996, **28**: 11 - 43.

[5] Osiptsov A N. Dusty-gas flow at the initial section of a plane channel and a circular tube[J]. *Izv Akad Nauk SSSR, Mekh Zhidk Gaza*, 1998, (6): 80 - 87. (in Russian)

[6] Healy D P, Young J B. Calculating of inertial particle transport using the Osiptsov Lagrangian method[A]. In: *Fourth International Conference on Multiphase Flow, ICMF* 2001[C]. New Orleans, May 27 - June 1, 2001, 1 - 12.

[7] Rudinger G. *Fundamentals of Gas-Particles Flow*[M]. Amsterdam: Elsevier, 1980.

[8] Chernyi G G. *Gas Flows at High Supersonic Velocity*[M]. Moscow: Fizmatgiz, 1959. (in Russian)

[9] Lunev V V. *Hypersonic Aerodynamics*[M]. Moscow: Mashinostroenie, 1975. (in Russian)

[10] Hayes W D, Probstein R F. *Hypersonic Flow Theory*[M]. New York: Academic Press, 1959.

[11] Carlson D J, Hoglund R F. Particle drag and heat transfer in rocket nozzles[J]. *AIAA Journal*, 1964, **2**(6): 1980 - 1984.